ELSEVIER

Nuclear Instruments and Methods in Physics Research A 491 (2002) 244–257

NUCLEAR INSTRUMENTS & METHODS IN PHYSICS RESEARCH Section A

www.elsevier.com/locate/nima

Application of digital sampling techniques to particle identification in scintillation detectors

L. Bardelli, M. Bini, G. Poggi*, N. Taccetti

I.N.F.N. and University of Florence, Via G. Sansone 1, Sesto Fiorentino, 50019 Italy

Received 25 March 2002; received in revised form 23 May 2002; accepted 18 June 2002

Abstract

In this paper, the use of a fast digitizing system for identification of fast charged particles with scintillation detectors is discussed. The three-layer phoswich detectors developed in the framework of the FIASCO experiment for the detection of light charged particles (LCP) and intermediate mass fragments (IMF) emitted in heavy-ion collisions at Fermi energies are briefly discussed. The standard analog electronics treatment of the signals for particle identification is illustrated. After a description of the digitizer designed to perform a fast digital sampling of the phoswich signals, the feasibility of particle identification on the sampled data is demonstrated. The results obtained with two different pulse shape discrimination analyses based on the digitally sampled data are compared with the standard analog signal treatment. The obtained results suggest, for the present application, the replacement of the analog methods with the digital sampling technique.

PACS: 29.40.M; 84.30.S; 25.70.Pq

Keywords: Digital; Identification; Phoswich; Detectors

1. Introduction

The identification of particles emitted in nuclear reactions in a wide range of kinetic energy, charge and, possibly, mass is an important feature requested by heavy ion experiments. The research in this field is mainly divided in two branches, not necessarily separated, one devoted to the development of new detectors, and the other concerning new methods of analysis.

Modern electronic sampling techniques (for example pipelining) have made it possible to design commercial high resolution ($\gtrsim 10$ bit) fast sampling analog to digital converters (ADC) which permit to retain the high precision of the standard analog methods (for instance for the energy measurement), while the detailed information achievable with signal sampling can be used in newly designed pulse shape discrimination applications. This may lead not only to better identification performances, but can also reduce

*Corresponding author. Tel.: +39-055-4572249; fax: +39-055-4572121.

E-mail address: poggi@fi.infn.it (G. Poggi).

0168-9002/02/$ - see front matter
PII: S0168-9002(02)01273-1

the complexity of the electronics in high granularity 4π experiments.

For applications of digital sampling techniques to nuclear detectors, see for instance Ref. [1].

In this work, a digital sampling and identification method has been developed and tested, with scintillation detectors, in the framework of the FIASCO experiment [2,3], devoted to the study of the reaction mechanism in heavy ion collisions at Fermi energies. The apparatus uses three different types of detectors to identify particles from $A = 1$ up to $A \simeq 100$: position sensitive parallel plate avalanche gas counters (PSPPAD) for the detection of heavy fragments (necessary for the event reconstruction and characterization), standard ΔE–E (200–500 μm) Silicon telescopes for heavy projectile residue and intermediate mass fragment (IMF) $2 < Z \lesssim 20$ identification, and scintillation phoswich detectors for both IMFs and LCPs.

The presented data have been collected during the second FIASCO campaign at the Laboratori Nazionali del Sud (LNS) facility in Catania (Italy).

2. Pulse shape identification techniques

The pulse shape discrimination (PSD) techniques exploit the dependence of the signal on the particle characteristics (energy, charge and mass). This method has been applied to signals coming either from a unique detector (Semiconductor Silicon or Scintillators) or from a composite one (as the phoswich scintillators used in this work). Examples involving a single detector are typically based either on the correlation of the signal risetime (often obtained with zero-crossing timing after a proper shaping) with its amplitude (in the case of Silicon detectors, see for instance [4–6]) or the correlation of partial integrals of the signal at different times. The second technique has often been applied to CsI(Tl) scintillators where a dependence of the fluorescence decay times and amplitudes is observed as a function of the ionization density, see for instance [7–9] and references therein. In the first kind of approach the timing information, usually involving time differences in the range of 1–50 ns, is obtained with purposely designed fast electronics and digitally stored by means of time to digital converters (TDC); the second approach is typically implemented by means of properly gated charge to digital converters (QDC) and can also be satisfactorily applied to composite scintillators, namely to phoswich detectors.

Using modern sampling techniques it is possible to digitize the output signal from a detector with high sample rate and good resolution: a detailed pulse shape analysis is possible on the sampled data, under the sole conditions that the information on the shape of the signal is well within the resolution and the Nyquist frequency of the used digitizer. The microprocessor-based on-line analysis that can be performed on the digitized data is another advantage with respect to the analog treatment, because complex and very effective algorithms like fast Fourier transforms, curve fitting, or even comparison with tabulated data can be easily implemented.

Recently, the feasibility of p/α-particle identification using digital pulse shape analysis has been demonstrated for small volume CsI(Tl) crystal in the low-energy ($\sim$MeV) region [9].

In the present work a fast digitizing system has been designed and build to sample signals from phoswich detectors and analyze their shape, replacing the aforementioned standard approach based on signal integration at different times. The method is proved to satisfactorily compete with the standard analog treatment, and allows for particle identification (p, d, t and from $Z = 1$ to ≈ 15) over a wide energy range ($E \lesssim 150$ AMeV).

3. The phoswich detector

The use of a stack of two different scintillation materials optically coupled to a single photomultiplier tube (PMT), known as *phoswich detector* (for implementations involving CsI(Tl), see Refs. [10–12]), is a standard method for particle identification (mainly light charged particles), typically implemented with gated QDC integrations at different times.

In the FIASCO experiment a non-standard three-layer phoswich configuration has been developed and used (see Fig. 1, upper panel): detailed

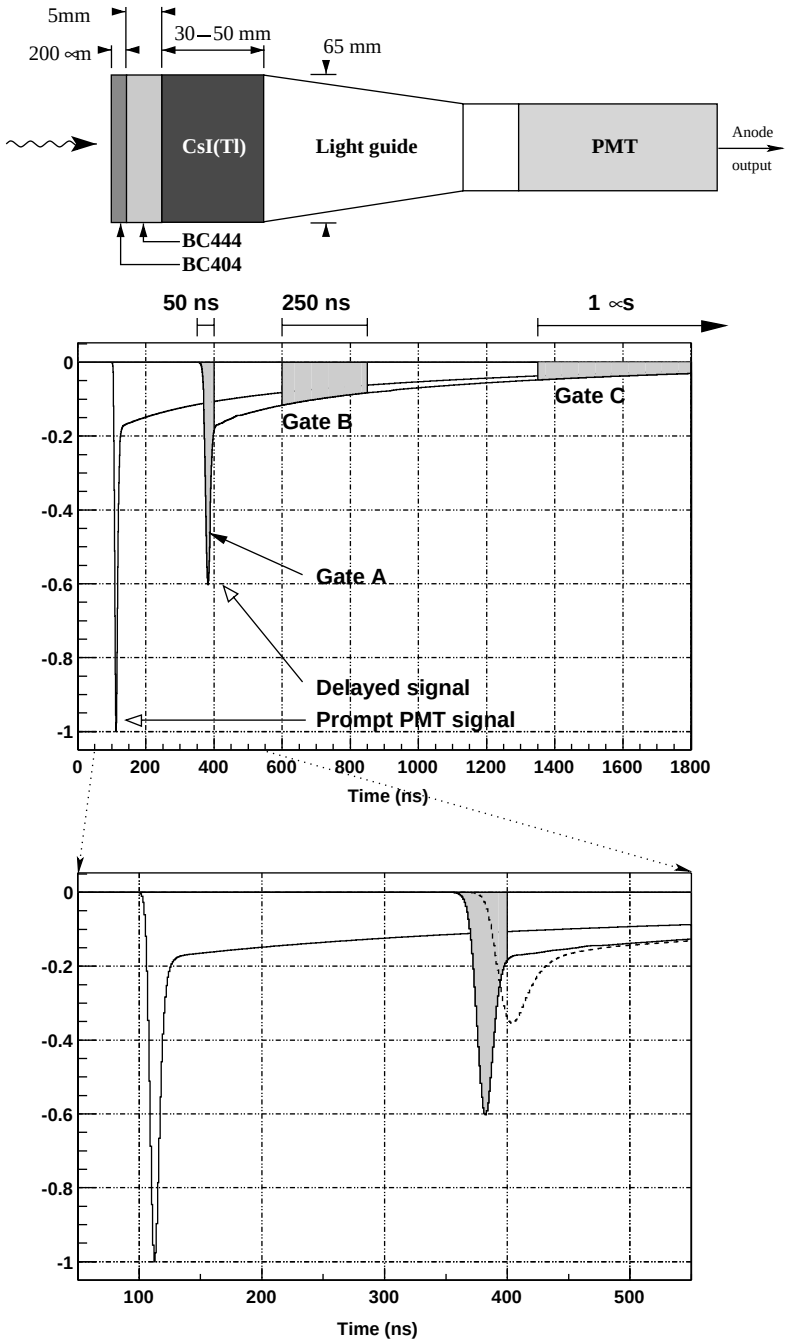

Fig. 1. Upper panel: geometrical characteristics of the phoswich detectors. Lower panels: calculation showing the effects of a 50 m composite transmission line on the PMT response; the three integration gates are also shown, as well as the effect of the antialiasing filter on the signal (dashed line, see Section 4.1 for details).

simulations and tests performed during the design phase [13,14] have shown the superiority of a three-layer phoswich detector over the standard two-layer configuration as far as the identification of particles from $Z = 1$ up to $Z \simeq 20$ is concerned. This configuration uses three different scintillators (BICRON BC404, BC444, and a CsI(Tl) crystal) coupled to a single PMT: the corresponding fluorescence decay times are equal to 1.8 ns, 180 ns and ~ 1 μs, respectively.

The anode output signal of this kind of detector results from the sum of three signals, their relative amplitudes being determined by the energy loss of the impinging particle in each scintillator: thus the shape of the current pulse reflects the type of the detected particle and can be used for identification purposes. In practice, the anode output is folded with the response of the photomultiplier and—in our case—of the 50 m long transmission line connecting the detectors placed in the scattering chamber to the electronics: in the lower panels of Fig. 1 a realistic phoswich signal is shown. Specifically, in the middle panel an example of prompt output signal from the photomultiplier is shown, assuming, for the sake of simplicity, similar contributions from the three scintillators to the total output pulse (the single photoelectron response of the photomultiplier has been taken into account). On the same panel the signal is shown as it appears after the transmission line, calculated with SPICE [15]. The used transmission line is a composite one, consisting in 5 m of RG58, followed by 40 m of RG213, ending with 5 m of RG58: it has been modeled using 500 RLC cells, with proper values of the components according to the cables' parameters. From the figure it is apparent (see also the bottom panel, where the time axis has been expanded) that the fastest component, associated with the 1.8 ns decay time of BC404, is actually smeared out over ~ 10–20 ns, mainly because of the transmission line response. In spite of the apparent deterioration in terms of high-frequency components with respect to the theoretical fluorescence output, it is nevertheless evident that a pulse shape analysis is still possible in order to discriminate amongst the various particles. Our standard approach for particle identification is described in the following subsection.

3.1. Pulse shape identification with analog methods

The usual analog approach consists in an integration of the anode signal at different times (as shown in Fig. 1), using standard QDC modules: a proper choice of width and delay with respect to the start of the current pulse (i.e. a Constant Fraction time-mark) of the integrations permits to obtain three quantities (indicated as Gate A, Gate B, Gate C in Fig. 1 and in the following) that are related to the energy loss of the particle in the three scintillators. Typically adopted values for the width (W) and the delay (D) of the three gates (see Fig. 1) are: $W_A = 50$ ns, $D_A = 0$ ns, $W_B = 250$ ns, $D_B = 250$ ns, $W_C = 1000$ ns, $D_C = 1000$ ns.

The correlations Gate A vs. Gate B and Gate B vs. Gate C provide the desired identification: for example in Fig. 2 (Gate A vs. Gate B correlation) it is possible to perceive the presence of lines corresponding to particles of different atomic number Z. The correlation Gate B vs. Gate C (not shown) permits the identification of particles with $Z = 1$ with good isotope resolution.

These results, which are satisfactory to the purpose of particle identification, demonstrate that the difference between the fluorescence times of the two fastest components is sufficiently large so that the shortest integration may last much longer than the original fast component decay time (50 ns with respect to few ns) and a good particle identification can still be observed. Besides, the slowing down of the fast component of the scintillation produces current signals which are less demanding in terms of linear dynamic range for the input stages of the front-end electronics.

In the next section, the digitizer developed for testing the feasibility of a digital pulse shape analysis with phoswich detectors is described.

4. The digitizer

A good resolution of the sampling system is needed in order to keep the wide dynamic range of the phoswich detector signal; besides, if the application is also aimed at performing particle identification, from the above discussion a

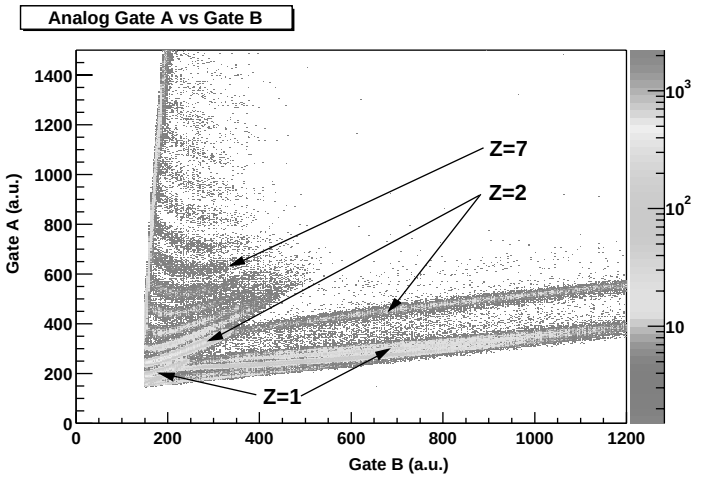

Fig. 2. Plot Gate A vs. Gate B obtained with a gated QDC integration of the anode signal from a phoswich detector: the presence of Z-lines, identifying the charge of the detected particles, is apparent.

sampling period much smaller than $W_A = 50$ ns is necessary, which means sampling rates significantly larger than ~ 20 Msamples/s. At the time of the design step of this task (March 2000), no commercial all-in-one board with suitable characteristics (resolution $\gtrsim 10$ bit, sample rate $\gtrsim 50$ Msamples/s) existed for use in on-line data acquisition,[1] so that a custom electronic board has been designed and build, based on the Analog Devices AD9432 analog to digital converter [16]: this chip is a 12 bit, 100 Msamples/s ADC, with differential analog input signal. Fast digitizer with similar characteristics are now commercially available. The AD9432 uses a pipelined conversion technique [17] to achieve both good resolution and high sample rate. Besides, the converted value at time t represents the input signal at time $t - T_{pipe}$ ($T_{pipe} = 100$ ns in our case): this makes it possible to record the whole leading portion of the signal without the need of external delays, like analog delays or digital circular buffers.

In Fig. 3, a schematic overview of the digitizer is given: each analog input signal (single-ended, directly from the PMT anode) is amplified, filtered

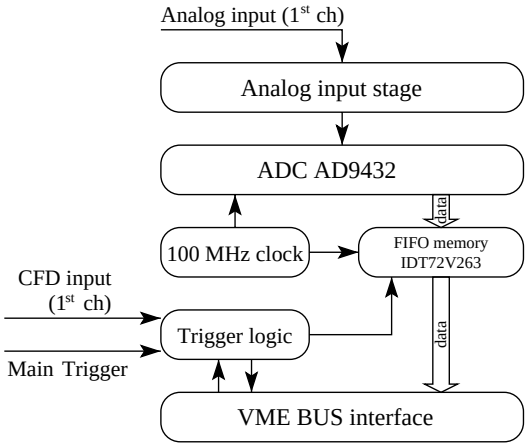

Fig. 3. Schematic overview of the custom board designed and used in this work: only one out of four identical acquisition channels is shown.

(see Section 4.1) and converted by a free running AD9432, which is controlled by a 100 MHz clock. The conversion rate is such that a direct readout from the VME bus is not possible: thus the standard solution of a FIFO memory (IDT72V263 [18]) to temporarily store the digital data has been adopted.

The system is also provided with an event validation logic: an external signal (the output of a Constant Fraction Discriminator associated with

[1] The requirements of sample rate and resolution can easily be met using digital oscilloscopes, but the very high cost/channel ratio and the low data transfer rate makes an on-line application unfeasible.

the detector) starts the write operation on the FIFO memory. If the event is not validated by the main trigger of the experiment within $\sim 1\,\mu s$ of waiting time, the transfer to the FIFO memory is stopped and the data are discarded; otherwise the transfer is continued up to the programmed length (of up to 2000 sample points) and, upon request, data are transferred to the main acquisition system via VME bus. The transferring and storing of the whole digitized waveform is impractical if applied to a large number of detectors: future applications (see Section 6) shall use a digital signal processor (DSP) to perform an on-line data analysis of each event. This solution, although of primary importance for large scale applications, was not necessary in the present work, aimed at studying advantages and drawbacks of the technique.

Four identical acquisition channels have been included in a single VME electronic board, which has been implemented in SMD technology with a six-layer double-side printed circuit; the trigger logic as well as the VME bus interface system have been implemented with complex electrically programmable logic devices (ALTERA EPM9320A [19]).

4.1. Analog section

The analog input section is provided with an antialiasing filter; moreover the single-ended signal from the detector has to be converted into a differential one, to satisfy the input requirements of the AD9432.

The complete schematic of the analog section, shown in Fig. 4, can be roughly divided into three parts: an amplifier with selectable gain, the low-pass antialiasing filter and a single-ended to differential section.

The amplifier section consists of an operational amplifier (`U1/A` in Fig. 4) in a non-inverting configuration: the operational amplifier (Analog Devices AD8044 [16]) has a 150 MHz gain-bandwidth product, with low noise characteristics

$$\left(\sqrt{\langle v_N^2\rangle/\delta f} = 16\mathrm{nV}/\sqrt{Hz},\ \sqrt{\langle i_N^2\rangle/\delta f} = 2\mathrm{pA}/\sqrt{Hz}\right).$$

A 3-pole antialiasing active filter has been adopted in order to minimize the distortion of the signal, which, in the present application of pulse shape analysis, should be kept as low as possible.

In Fig. 5, the results of a calculation of three standard different active filters are shown (Butterworth, Chebychev and Bessel) both in time (part a) and frequency domain (part b). The calculations have been done with the SPICE simulator [15], and realistic models (Analog Devices) for the operational amplifiers. The cutoff frequency has been fixed to 15 MHz for all the filters. Because of its better performance in terms of constant delay (corresponding to smaller signal distortion), the Bessel filter has been chosen. The antialiased signal is shown in Fig. 1 (bottom panel, dashed line): although, as expected, the fast component is spread over a somewhat larger time interval, the overall shape of the signal is preserved.

With the adopted layout, the amplifier section and the antialiasing filter for two independent channels are implemented with a single AD8044 (quad op-amp).

The filtered signal has to be transformed to match the input requirements of the analog-to-digital converter, that needs a differential input with a common-mode voltage of about 3 V on both inputs. The Analog Devices AD8138 operational amplifier [16] is well suited for this purpose, being a differential op-amp with a common mode output voltage adjustable via a DC voltage applied to the `VOCM` pin.

Since the detector signals are unipolar, the analog section has been designed in order to exploit the whole dynamic range of the converter (1 V differential, for AD9432). In fact, instead of using a symmetric configuration for the two output signals (`R7` = `R10` in Fig. 4), an asymmetric configuration has been used (`R7`$\neq$`R10`), effectively extending the dynamic range for unipolar signals.

The bandwidth-integrated noise of the analog electronic section σ_v has been determined, for gain = 1, by comparing the digitized experimental data for zero input signal with simulations. Namely, the sampling process has been simulated, for different figures of the analog noise σ_v, taking into account the quantization effect of the sampling process, the baseline subtraction (see Section 5.1) and the specified signal to noise ratio of the ADC: the best agreement between the

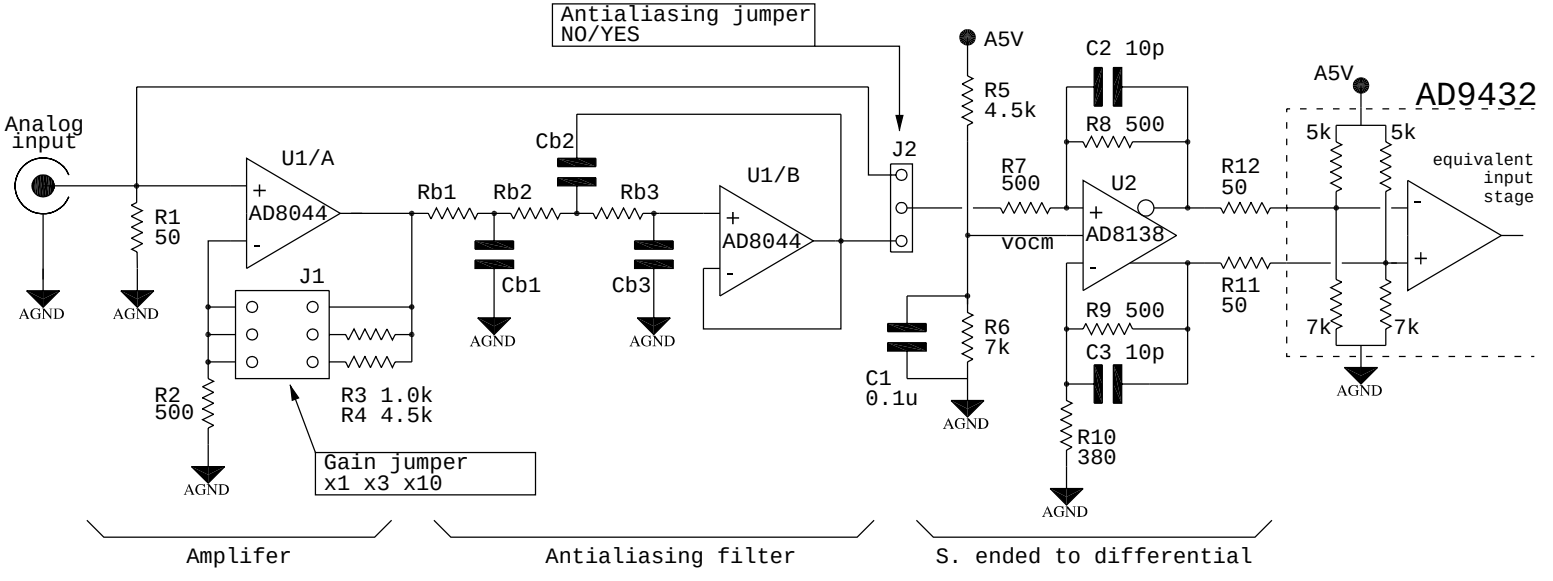

Fig. 4. Schematic of the analog input stage used in the digitizer: from left to right the main amplification stage (with jumper-variable gain), the active filter, the single-ended to differential converter, and the equivalent input stage of the analog to digital converter.

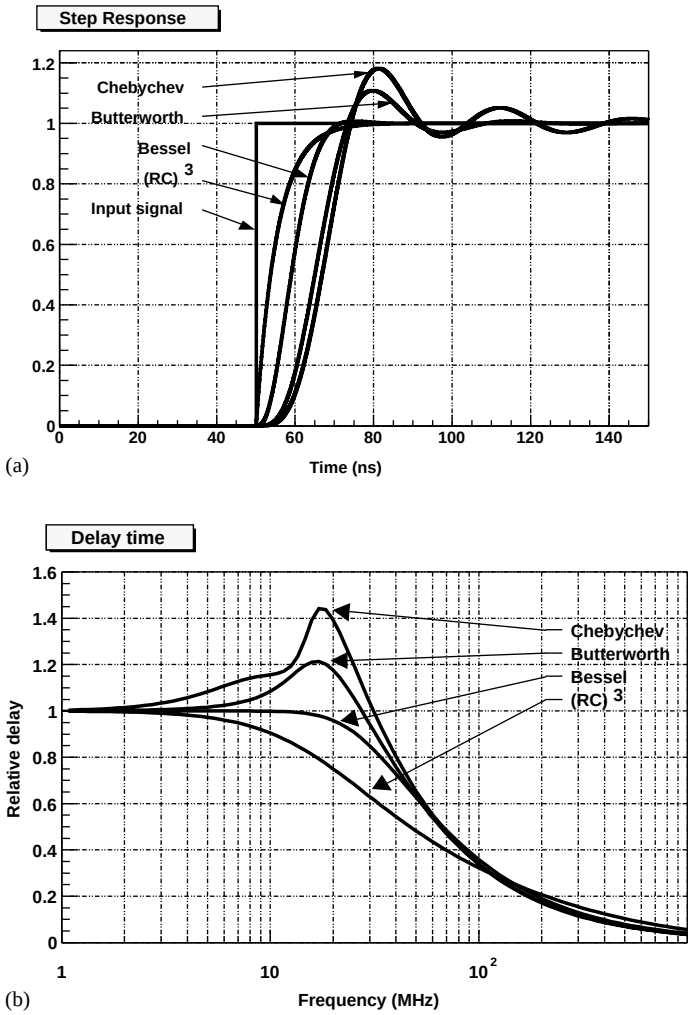

Fig. 5. Comparison of the time response to the step function (part a) and of delay time (normalized to DC value, part b) as a function of frequency for different active filters with the same cutoff frequency (a three-pole RC filter is also shown for comparison).

experimental and the simulated distributions has been found for $\sigma_v = 120\,\mu V$ (referred to the "analog input" of Fig. 4) with a normalized $\chi^2 \simeq 0.7$.

5. Application to phoswich detectors

5.1. Pulse shape identification with digital methods

The digitizer previously described has been used to sample the output of a phoswich detector: two different (off-line) analyses have been developed and tested, both being well suited for future on-line DSP-based data taking and elaboration.

As a first step of the analysis, in both methods a baseline subtraction algorithm is applied to the data, to eliminate undesired low frequency components (for example the 50 Hz pick-up): each signal has been sampled for 20 μs, a time interval significantly longer than any fluorescence decay time of the scintillators. In this way, the ending portion of the digitized data is used for determining the baseline (average over the sample points in

the last 5 μs), which must be subtracted. Using the very first samples preceding the rising edge of the signal, it is possible to check the baseline stability and to possibly reject partially piled-up events.

In order to perform the analyses described in the following, a precise value of the starting time of the detector signal is needed. In principle, the data are synchronous with the CFD mark which triggers the acquisition. However, the 10 ns uncertainty associated with the asynchronous clock of the conversions is too large for the required application and a more precise time mark is computed as the instant in which the conversions reach a preset constant fraction (20%) of the maximum amplitude. Linear interpolation between the sample points has been used to improve the accuracy of the determination of the starting time from ~ 10 ns (the sampling period) to $\lesssim 3$ ns.

5.1.1. Digital integration

The first kind of analysis is based on three numerical integrations of the sampled signal: it can then be simply regarded as the digital equivalent of the analog technique previously described.

The time mark extracted from the data is used as a reference to properly gate the integrations. The width of the first integration zone (that we still call Gate A) has been somewhat extended with respect to the analog integration, in order to maintain the full coverage of the fast component after the antialiasing filter. The integrations are carried out using trapezoids, with linear interpolation between sample points at the extremes. The interpolation is necessary mainly for the narrowest gate, because of the low number of available sampled points (10 for a 100 ns wide gate). The identification can then be performed exactly in the same way as for the analog treatment. A correlation like that shown in Fig. 2 is build and used for particle identification. In Section 5.2 a quantitative comparison between this method and the analog one will be discussed.

5.1.2. Look-up table

Using the large amount of information available for each event, a relatively more elaborate method of analysis has been devised and successfully tested, based on a linear fit of the detector signals with experimentally determined functions. At variance with the approach presented in the preceding section, this method cannot be implemented with an analog treatment of the signal.

Following the discussion of Section 3, the anode signal can be written as

$$\mathbb{S}(t) = \mathscr{A} \cdot f_{\mathrm{A}}(t) + \mathscr{B} \cdot f_{\mathrm{B}}(t) + \mathscr{C} \cdot f_{\mathrm{C}}(t) \tag{1}$$

where f_{A} is the response of the system to the first scintillator, f_{B} to the second, f_{C} to the third (the indexes A, B and C refer from now on to the three scintillators BC404, BC444 and CsI(Tl), respectively). In Eq. (1) these functions are supposed to be known: a method for experimentally obtaining these response functions will be presented later. $\mathscr{A}$, $\mathscr{B}$ and $\mathscr{C}$ in Eq. (1) are unknown parameters related to the energy loss of the particle in the three scintillators and, if measured, they can be used for identification, by plotting $\mathscr{A}$ vs. $\mathscr{B}$ and $\mathscr{B}$ vs. $\mathscr{C}$. Assuming f_{A}, f_{B} and f_{C} to be known functions, each signal $S(t)$ can be fitted with a least square method (N is the number of sample points):

$$M = \sum_{i=1}^{N} [S(t_i) - \mathbb{S}(t_i)]^2. \tag{2}$$

This is a *linear* fit in the unknown parameters $\mathscr{A}$, $\mathscr{B}$ and $\mathscr{C}$.

The function $f_{\mathrm{A}}(t)$ can be obtained noting that in the experimental correlation build with the sampled data Gate A vs. Gate B there is a region of events with Gate B $\simeq 0$ and Gate A $\neq 0$:[2] these are events in which the impinging particle has been fully stopped in the fast scintillator "A". As a consequence, each of these signals is proportional to f_{A}: their sum (taking into account their different starting times) gives an almost noiseless determination of f_{A}. In Fig. 6, an example of reconstructed f_{A} function is given: it develops over a time span of ~ 100 ns (mainly due to the transmission line and to the antialiasing filter time constant), whereas the light pulse from the fast scintillator BC404 extends in the ns range ($\tau_{\mathrm{A}} = 1.8$ ns). Obviously, f_{B} and f_{C} differ from f_{A} because of the different fluorescence decay time and not for the electronic treatment. Because of its short

[2] This region can easily be seen in Fig. 2, if the QDCs pedestals are properly taken into account.

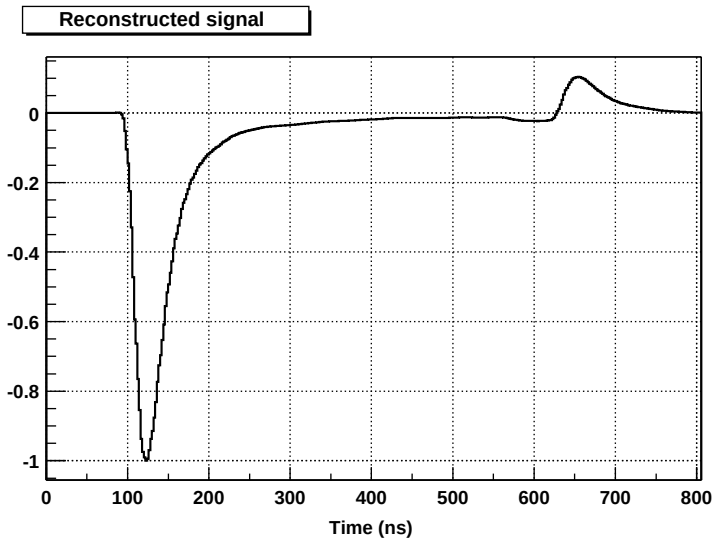

Fig. 6. Experimentally reconstructed (amplitude normalized) f_A signal: see text for explanations.

duration, the fast scintillator component can be treated as the δ-impulse excitation and f_A approximates the response function of the system: therefore f_B and f_C can be obtained with a folding integral of f_A with a function like $\exp(-t/\tau)$, with $\tau = \tau_B, \tau_C$ corresponding to the decay constant of the relevant scintillator "B" or "C". The following results have been obtained using $\tau_B = 180$ ns and $\tau_C = 1$ μs. The obtained reference functions f_A, f_B and f_C can then be used to fit *all* the sampled signals with Eq. (2). In this approach it has been assumed that the response of the slower scintillators can be described by a pure exponential behavior; an extension of the method to take into account the presence of more than one fluorescence component is straightforward (see next paragraph).

This *experimental* determination of the functions f_A, f_B and f_C makes it possible to consider all the operating conditions of the system, including the characteristic response of each detector, details and flaws of the electronic set-up (as the impedance mismatch in the transmission line present in Fig. 6), which could hardly be included if only simulations were used for determining the response functions.

The method has been developed, taking into account the constraints imposed by future DSP-based applications: the three reference functions can be stored in memory during the initialization (for example in a look-up table); the fitting procedure, which is linear in the unknown parameters $\mathscr{A}$, $\mathscr{B}$ and $\mathscr{C}$, can be very fast, because it is closed (non-iterative) and mainly consists in summations over data points.

For each fit, as usual, the sum of residues can be used to estimate the goodness of the fit: this makes it easy to check the dependability of the procedure on an event-by-event basis (for example a pile-up rejection algorithm is straightforward).

This method can be implemented in a self contained procedure totally based on the digital sampling approach. A possible initialization procedure may develop as follows: in a first run one collects some data and the digital integration is applied, so that the Gate A vs. Gate B correlation is built; the correlation permits to select events from which f_A is determined, as well as f_B and f_C, as described before.

5.2. Comparison between analog and digital methods

Both the proposed identification methods based on digitally sampled data have been tested: moreover, using a 50 Ω splitter, in each event the signal

from the phoswich detector has been simultaneously fed to both the analog (QDC-based) and the digital electronic chains. This approach allowed us to directly compare the different techniques.

In Fig. 7, the identification spectra obtained by proper linearization of the correlation Gate A vs. Gate B and Gate B vs. Gate C (analog and digital integrations) and of the correlation $\mathscr{A}$ vs. $\mathscr{B}$ and $\mathscr{B}$ vs. $\mathscr{C}$ (*look-up table*) are shown.

From the Gate A vs. Gate B—and $\mathscr{A}$ vs. $\mathscr{B}$—based identification spectra, it is apparent that the analyses performed with the digital sampling of the data provide a discrimination as good as the one obtained with the analog technique. We have verified that the quality of the results for the digital integration is not very sensitive to the width of the first integration: variations from about 50 up to 200 ns do not significantly influence the final identification results. In the region $Z > 10$, the

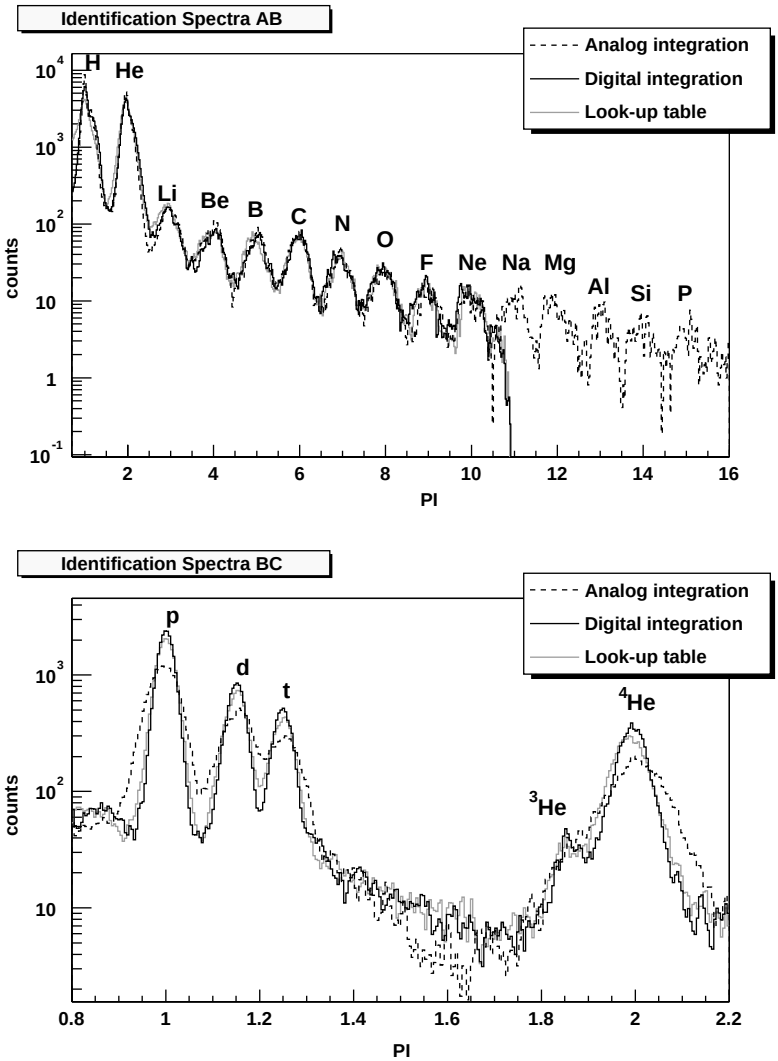

Fig. 7. Identification spectra obtained by linearizing the correlation Gate A vs. Gate B, Gate B vs. Gate C (analog and digital integrations), $\mathscr{A}$ vs. $\mathscr{B}$ and $\mathscr{B}$ vs. $\mathscr{C}$ (*look-up table*). The different methods are discussed in the text.

digital identification is missing simply because of the ADC overflow: in fact, the detected high-Z particles experience a large energy loss in the fast scintillator and this implies a large output signal, causing an overflow of the ADC (only signals up to ~ 1 V are accepted in the present configuration). In future applications, a 6 dB attenuation of the input signal will be included, which is expected—according to simulations which have been performed—to sufficiently increase the dynamic range of the Z-identification, without deteriorating its quality.

On the other side, the identification obtained from the Gate B vs. Gate C and $\mathscr{B}$ vs. $\mathscr{C}$ correlations clearly shows that a better discrimination is obtained with both the proposed digital analyses (note the logarithmic scale of Fig. 7). The overall peak/valley ratio is improved with respect to the analog method.

A quantitative comparison between the methods can be performed using the Factor of Merit (FoM) of the discrimination, as defined in Ref. [20]. In Table 1, the results obtained with the three methods are shown (the best value of each row has been highlighted). The digital methods improve the identification from the Gate B vs. Gate C correlation by a factor ~ 2 with respect to the analog integration results.

The *look-up table* method deserves a little discussion: namely it may seem surprising that such a method, in principle capable of better exploiting the whole collected information, does not give correspondingly better discrimination results with respect to the digital integration approach and rather behaves slightly worse. In order to possibly improve the obtained discrimination, a second component in the CsI(Tl) fluorescence (a fourth term in Eq. (2)) was introduced; tests have been done by varying the values of the two CsI(Tl) fluorescence time-constants over the known values reported in the literature (see for instance Ref. [21]). The so obtained results did not show any improvement in the quality of the discrimination. We presently believe that this result has to be associated with the following facts:

- the particle discrimination in all the presented cases is mainly due to the signal sharing between plastic and inorganic scintillators, thus resembling a ΔE–E technique rather than a proper Pulse Shape Analysis on the CsI(Tl) scintillator; the details of the slow CsI(Tl) components thus play a minor role in the overall discrimination;
- as mentioned before, the *look-up table* approach forces one to describe the detector response in terms of functions where the *to-be-fit* parameters have to appear linearly. This implies in any case a somewhat crude description of the CsI(Tl) response: in particular it prevents the possibility of fitting not only the amplitudes of the different components but also the values of the fluorescence time-constants which are known to strongly depend on the particle species and their energy [10,21];
- for the sake of clarity and comparison with the other methods, the presented identification is performed in a two-dimensional correlation scheme between the fitted parameters. It seems advisable to check whether different linear combinations or even multi-dimensional correlation between $\mathscr{A}$, $\mathscr{B}$ and $\mathscr{C}$ (and possibly a fourth component) are capable of a better discrimination. In this respect, it is to be noted that the digital (and analog) integration methods actually discriminate the particle exploiting the correlation among two differently weighted sum of $\mathscr{A}$, $\mathscr{B}$ and $\mathscr{C}$.

Table 1
FoM results for the three identification methods (Analog integration, Digital integration, Look-up table), obtained for various particle pairs

	FoM		
Particle Pair	Analog	Digital	Look-up
H–He •	**1.57**	1.42	1.27
Z–$Z+1$ ($Z>1$) •	0.8–1.0	0.8–1.0	0.8–1.0
p–d ★	0.93	**1.66**	1.39
d–t ★	0.51	**1.04**	0.85
p–He ★	4.61	**8.27**	6.85

Data marked with • has been obtained via Gate A vs. Gate B identification spectra (top of Fig. 7), whereas ★ refers to Gate B vs. Gate C (bottom of Fig. 7).

Extension and studies of different discrimination methods, involving multi-dimensional correlation between the fitted parameters are presently under investigation; however, they are believed to be beyond the limits of the present work, mainly intended to demonstrate the feasibility of the *look-up table* approach, as an example of a fast fitting procedure, which takes into account explicitly the details of the electronic response of the system, implements an on-line processing of the data and satisfies the particle discrimination requirements of our experiment.

Although the presented results refer to one selected channel of the four implemented on the digitizer board, all the channels show results of the same quality.

6. Future developments

Future developments of this work will include the use of a DSP for on-line analysis of the signals: the system, currently under design and test, is based on the Analog Devices ADSP-2189M, a fixed point, low cost Digital Signal Processor with a 13.3 ns instruction cycle time. The full digitizing-DSP system has a modular architecture: each acquisition channel (analog section, ADC, FIFO, DSP and glue logic) is mounted on a separate small-sized printed circuit board (PCB). The VME interface is implemented on a single ''mother-board'', provided with connectors for up to 16 channels. This structure allows for a quick development and easy upgrading of the system. Each DSP will be individually programmable at run-time through the VME bus.

Applications of our digitizer to other detectors are in progress, also in connection with extensions of the *look-up table* method: namely, preliminary tests are under way on ion-implanted and neutron transmutation doped Silicon detectors, with rear side injection of particles, with encouraging results.

7. Conclusions

In the present work, a study of the applicability of digital sampling methods to particle identification techniques has been performed.

A digitizer has been purposely developed, using 100 Msamples/s, 12 bit analog to digital converters: the 3-pole active antialiasing filter employed has shown low distortion and good noise performances.

The sampling method has been applied to the three-layer phoswich detectors used in the FIASCO experiment: two different analyses on digitized data have been performed, and the quality of the obtained particle identification has been compared with the results of the analog method. This comparison, performed on the *same* set of events, shows that the digital sampling technique is characterized by equal or better identification performances with respect to the analog methods. Moreover, practical considerations, like cabling complexity, cost of the electronic chain and versatility in terms of signal treatment and elaboration, make the digital approach method very appealing for the application to large experimental setups.

Acknowledgements

Many thanks are given to P. Calonaci, R. Ciaranfi, M. Grandi and M. Montecchi for their skillful technical support and to G. Pasquali for helpful discussions.

References

[1] G.F. Knoll, Radiation Detection and Measurement, 3rd Edition, Wiley, New York, 1999, p. 647.
[2] G. Casini, et al., Eur. Phys. J. A 9 (2000) 491.
[3] S. Piantelli, et al., Phys. Rev. Lett. 88 (2002) 052701.
[4] J.B.A. England, G.M. Field, T.R. Ophel, Nucl. Instr. and Meth. A 280 (1989) 291.
[5] M. Mutterer, et al., IEEE Trans. Nucl. Sci. 47(3) 2000.
[6] G. Pausch, et al., Nucl. Instr. and Meth. A 365 (1995) 176.
[7] G. Viesti, et al., Nucl. Instr. and Meth. A 252 (1986) 75.
[8] W.G. Gong, et al., Nucl. Instr. and Meth. A 268 (1988) 190.
[9] W. Skulski, M. Momayezi, Nucl. Instr. and Meth. A 458 (2001) 759.
[10] J. Alarja, et al., Nucl. Instr. and Meth. A 242 (1986) 352.
[11] D.W. Stracener, et al., Nucl. Instr. and Meth. A 294 (1990) 485.

[12] R.T. De Souza, et al., Nucl. Instr. and Meth. A 295 (1990) 109.
[13] L. Bidini, Diploma thesis, University of Florence, 1999, unpublished.
[14] S. Piantelli, Ph.D. Thesis, University of Florence, 2000. Unpublished.
[15] T. Quarles, A.R. Newton, D.O. Pederson, A. Sangiovanni-Vincentelli, SPICE3 Version 3f3 User's Manual, University of California, 1993.
[16] Analog Devices, WEB site www.analog.com.
[17] P. Horowitz, W. Hill, The Art of Electronics, Cambridge University Press, Cambridge, 1989.
[18] Integrated Device Technology, WEB site www.idt.com, IDT72V263's datasheet.
[19] ALTERA, web-site www.altera.com, MAX9000 family's datasheet.
[20] R.A. Winyard, J.E. Lutkin, G.W. McBeth, Nucl. Instr. and Meth. 95 (1971) 141.
[21] F. Benrachi, et al., Nucl. Instr. and Meth. A 281 (1989) 137.